AGU PUBLICATIONS

Journal of Advances in Modeling Earth Systems

RESEARCH ARTICLE
10.1002/2014MS000381

Exploratory analysis of extremely low tropical cyclone activity during the late-season of 2010 and 1998 over the western North Pacific and the South China Sea

Haikun Zhao[1], Pao-Shin Chu[2], Pang-Chi Hsu[1], and Hiroyuki Murakami[3,4]

[1]Pacific Typhoon Research Center, Key Laboratory of Meteorological Disaster of Ministry of Education, CDRC/ESMC, International Laboratory on Climate and Environment Change, Nanjing University of Information Science and Technology, Nanjing, China, [2]Department of Atmospheric Sciences, School of Ocean and Earth Science and Technology, University of Hawaii, Honolulu, Hawaii, USA, [3]Geophysical Fluid Dynamics Laboratory, Princeton University, Princeton, New Jersey, USA, [4]Meteorological Research Institute, Tsukuba, Japan

Key Points:
- Unusually low TC activity in 2010 and 1998 has received less attention
- To understand how the regional SST anomalies modulate circulations
- Better understanding of factors affecting tropical cyclone activity

Correspondence to:
H. Zhao,
zhk2004y@gmail.com

Citation:
Zhao, H., P.-S. Chu, P.-C. Hsu, and H. Murakami (2014), Exploratory analysis of extremely low tropical cyclone activity during the late-season of 2010 and 1998 over the western North Pacific and the South China Sea, *J. Adv. Model. Earth Syst.*, *06*, doi:10.1002/2014MS000381.

Received 4 SEP 2014
Accepted 17 OCT 2014
Accepted article online 24 OCT 2014

Abstract This study attempts to understand why the tropical cyclone (TC) frequency over the western North Pacific and the South China Sea was so low in 2010 and 1998 even though a strong La Niña signal occurred in both years. We found that the TC frequency during the late-season (October to December), not in the peak season (July to September), makes 2010 a record low year; the next lowest year is 1998. Specifically, four TCs were observed over the South China Sea (SCS) in the late-season of 1998, but no TCs occurred over the SCS in the same season during 2010. The genesis potential index is used to help diagnose changes in environmental conditions for TC genesis frequency. Results indicate that the decreased low-level vorticity makes the largest contribution to the decreased TC formation over the SCS. The second largest contribution comes from the enhanced vertical wind shear, with relatively small contributions from the negative anomaly in potential intensity and reduction in midlevel relative humidity. These observational results are consistent with numerical simulations using a state of the art model from the Meteorological Research Institute (MRI-AGCM 3.2 Model). Numerical experiments show that the unfavorable conditions for sharply decreased TC formation during the late-season over the SCS in 2010 mainly results from the sea surface temperature anomaly over the western North Pacific basin. This effect is partly offset by the sea surface temperature anomaly in the South Indian Ocean and Northern Indian Ocean basins.

1. Introduction

Tropical cyclones (TCs), which are characterized by strong winds and torrential rain, are the most disastrous weather systems and thus are a major focus for tropical meteorology. The possibility of great destruction and economic hardship brought about by TCs also makes them a serious concern for affected countries as well. The western North Pacific (WNP) basin stands out as the most active TC genesis region. On average, the WNP basin, which includes the South China Sea (SCS), experiences about 26 TCs each year based on the Joint Typhoon Warning Center (JTWC) best track data set, accounting for around 33% of TCs worldwide. Previous studies have suggested that WNP TC activity is strongly influenced by various modes of natural climate variability, such as intraseasonal oscillations [*Liebmann et al.*, 1994; *Kim et al.*, 2008; *Huang et al.*, 2011; *Li and Zhou*, 2013], interannual variation [*Dong*, 1988; *Lander*, 1994; *Chen and Weng*, 1998; *Chan*, 1985, 2000; *Wang and Chan*, 2002; *Chia and Ropelewski*, 2002; *Chu*, 2004; *Camargo and Sobel*, 2005; *Camargo et al.*, 2007; *Zhao et al.*, 2010, 2011], as well as decadal and interdecadal variability [*Yumoto and Matsuura*, 2001; *Yumoto et al.*, 2003; *Ho et al.*, 2004; *Chan*, 2008; *Liu and Chan*, 2008; *Yokoi and Takayabu*, 2013; *Zhao et al.*, 2014; *Hsu et al.*, 2014].

On the interannual time scale, the El Niño-Southern Oscillation (ENSO) is well recognized as the most important factor affecting WNP TC activity. Although the total TC frequency over the WNP basin does not change appreciably from El Niño to La Niña years, TC intensity during El Niño years is stronger than that during La Niña years, which is mainly due to significantly enhanced TC formation in the southeast quadrant of the WNP basin during strong El Niño years. The El Niño provides a favorable environment that leads to TCs with longer lifetimes and higher intensity over the warmer ocean [*Wu and Lau*, 1992; *Wang and Chan*, 2002; *Camargo and Sobel*, 2005; *Wu and Wang*, 2008; *Zhao et al.*, 2011, 2014].

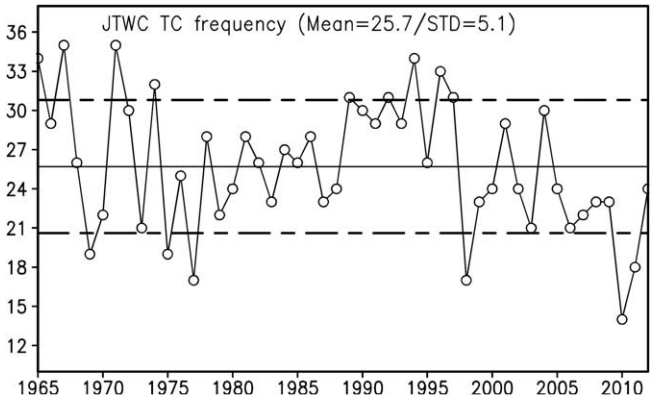

Figure 1. Annual TC count during the period 1965–2012 from the Joint Typhoon Warning Center (JTWC) best track data set. The solid line represents the climatological mean of TC count. Dashed lines stand for one standard deviation of TC count during the period 1965–2012.

In this study, TCs with a maximum sustained surface wind speed of 35 knots or above are considered. Since weather satellites began routine monitoring in 1965, we will use the JTWC best track records over the last 48 years. As shown in Figure 1, there is a pronounced interannual variability in WNP TC frequency with a mean of about 26 TCs and standard deviation of about five TCs during the period 1965–2012. The 14 TCs observed in 2010 is the lowest TC record since 1965 and is more than two standard deviations away from the mean. This is followed by 17 TCs in 1998. These results are also found in the other two best track data sets (i.e., JTWC, JMA—the Regional Specialized Meteorological Center of Japan Meteorological Agency and CMA_STI—the Shanghai Typhoon Institute of China

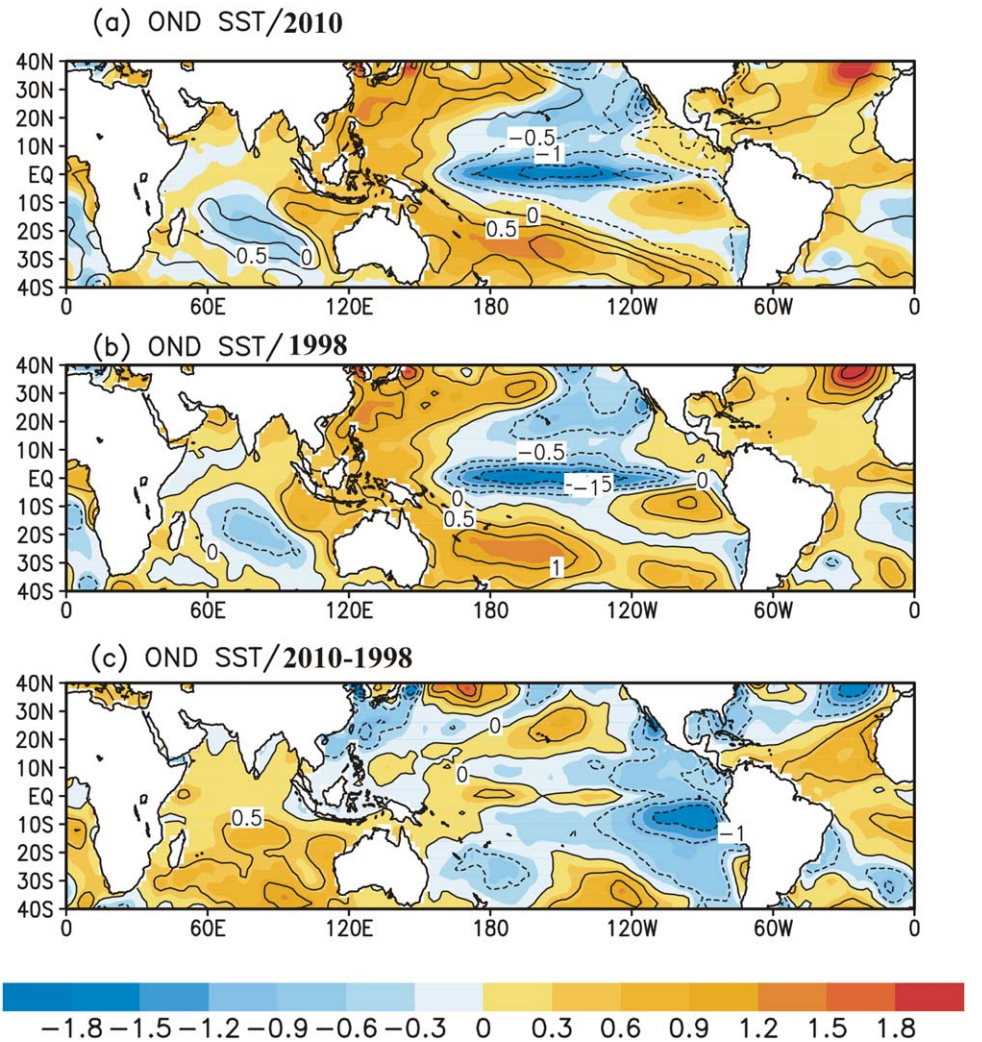

Figure 2. Anomalous late-season SST distributions in (a) 2010 and (b) 1998 compared to the climatology (1965–2012) and (c) their difference. Unit: K.

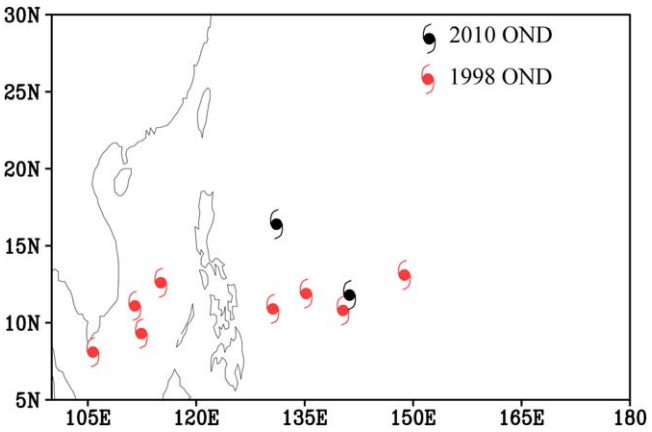

Figure 3. Tropical cyclone genesis locations during the late-season for 1998 (red) and 2010 (black).

Meteorological Administration), suggesting that the record low annual TC counts in 2010 and 1998 are robust and not a spurious fact due to observational techniques.

Previous studies have also discussed the decrease in TC activity during the recent decade or so [*Maue*, 2011; *Liu and Chan*, 2013]. To our knowledge, the unusually low TC activity in 2010 and 1998 has not received much attention. As shown in Figures 2a and 2b, for both years a strong La Niña event developed in the late-season (October to December). However, because there is no robust relationship between ENSO and WNP TC number, it is a puzzle as to why 2010 and 1998 could lead to extremely low TC activity. It is thus of interest to understand the causes of the inactive TC activity in these 2 years and what led to the even lower TC number in 2010.

To examine whether the inactive TC activity occurs in a specific season, the TC genesis number during different seasons are compared. During the preseason (January to June), only one TC was reported in 2010 while none occurred in 1998. During the peak season (July to September), 11 TCs occurred in 2010, which is about four less than the average number but slightly more than 1998 (nine TCs). For the late-season, only two TCs formed in 2010, in stark contrast to eight TCs in 1998. Apart from the difference in TC frequency in the late-season between 1998 and 2010, the significant difference in TC genesis locations over the SCS is also noteworthy (Figure 3). In the late-season of 1998, there are four TCs over the SCS but none in 2010. Moreover, a moderate difference is also found over the Philippines Sea (four TCs in 1998 versus two TCs in 2010).

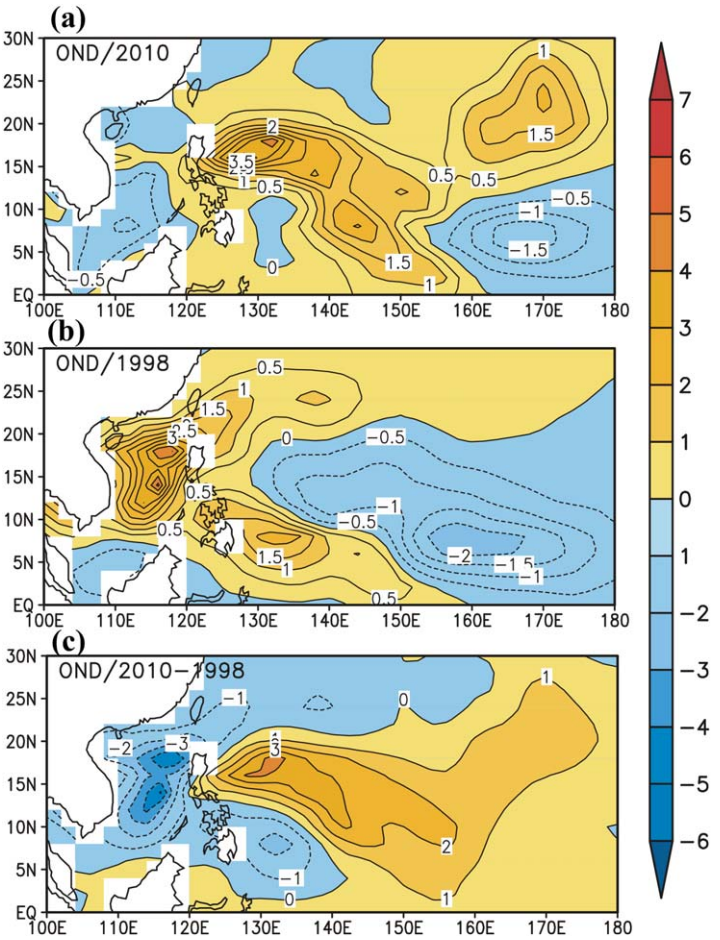

Figure 4. Anomalous GPI of (a) 2010 and (b) 1998 and (c) their difference during the late-season. Analysis is based on the NCEP/NCAR reanalysis I data set.

The extremely low TC activity over the WNP may be associated with the atmospheric circulation in response to the tropics-wide sea surface temperature (SST) change because of the effect of remote and local SST changes in controlling TC activity [*Wu and Lau*, 1992; *Emanuel*, 2005; *Vecchi and*

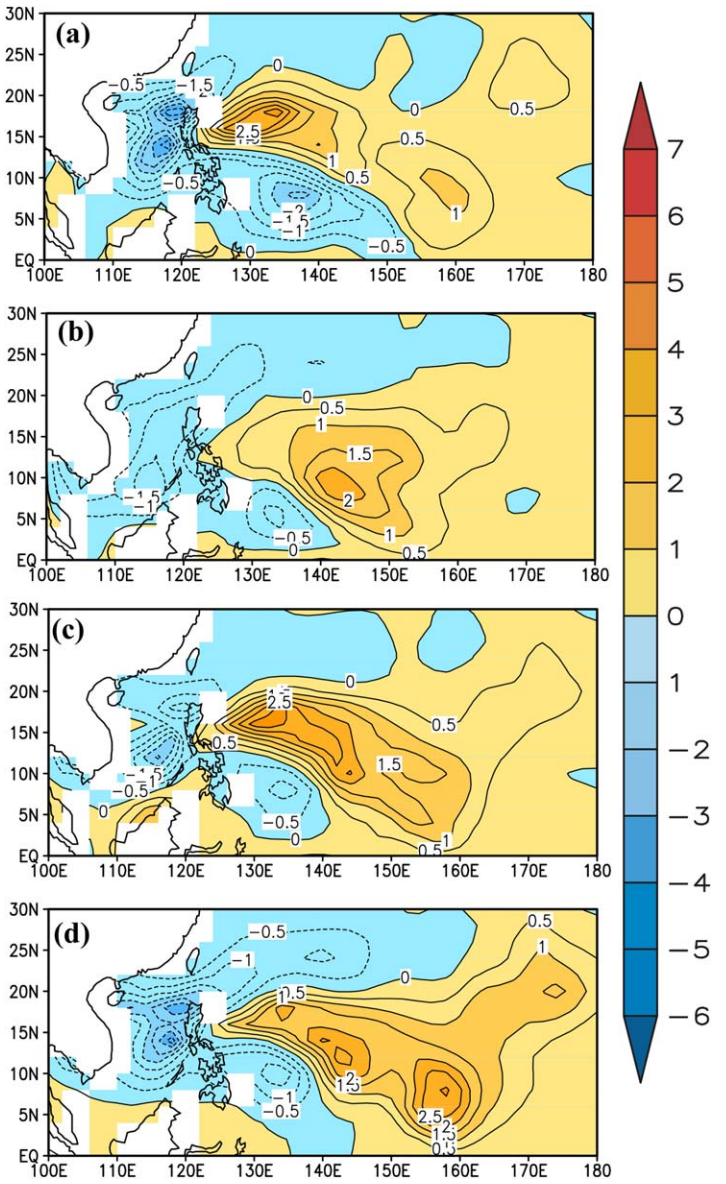

Figure 5. Relative contributions of (a) vertical wind shear, (b) potential intensity, (c) midlevel relative humidity, and (d) low-level absolute vorticity to the total difference of anomalous GPI (2010 minus 1998) during the late-season.

Soden, 2007; *Latif et al.*, 2007; *Knutson et al.*, 2008; *Hsu et al.*, 2014]. At first glance, the anomalous SST pattern between the late-season of 2010 and 1998 in Figures 2a and 2b bears a La Niña signal and is similar. However, there are considerable differences in the magnitude of SST anomalies when 2010 is compared to 1998 (Figure 2c). These include cooling over a major portion of the WNP, negative SST anomalies over the equatorial eastern Pacific, and positive SST anomalies over the Indian Ocean and some portions of the Pacific. Because SST changes over the different ocean basins can induce variations of large-scale atmospheric circulation and thus affect TC activity [*Du et al.*, 2011; *Zhan et al.*, 2011; *Tao et al.*, 2012], we will also investigate the relative roles of regional SST distribution in the context of understanding the physical mechanisms leading to the record low TC genesis of 2010 and 1998.

In this study, our purpose is to examine why the TC frequency is low during the late-season in 2010 even though SST patterns are similar to 1998. The influence of large-scale conditions and regional SST changes over different oceans related to TC activity during the late-season is emphasized to shed light on the lowest recorded TC number in 2010. The remainder of the paper is organized as follows. Section 2 describes the data and methodology used in this study. The large-scale dynamic and thermodynamic anomalies associated with record low TC activity during the late-season in 2010 and 1998 are analyzed and compared in section 3. The role of regional SST changes during the late-season is examined in section 4 using numerical model experiments. This is followed by a summary in section 5.

2. Data and Methods

2.1. Data

There are several organizations that maintain their own historical TC records for the WNP basin. These include the JTWC, JMA, the Hong Kong Observatory (HKO) of China, and CMA_STI. Previous studies have suggested that the difference in TC tracks are generally small, particularly in the satellite area, while the

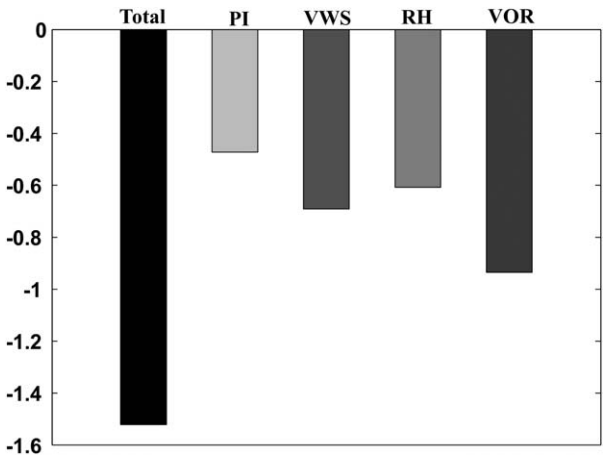

Figure 6. Differences (2010 minus 1998) of the total GPI and varying potential intensity, vertical wind shear, relative humidity, and vorticity during the late-season over the SCS (5–20°N, 105–120°E).

intensity records derived from these data sets were quite different from various TC best track data sets [*Wu et al*., 2006; *Emanuel et al*., 2008; *Song et al*., 2010; *Ren et al*., 2011; *Wu and Zhao*, 2012]. The uncertainty involved in TC data sets has become an important issue in understanding the possible influence of climate change on TC activity. *Kamahori et al*. [2006] reported large differences in the number of intense TCs (Cat4–5) during 1991–2004 in JTWC and JMA best track data sets, but the total TC numbers between them are not very different. *Chan* [2008] suggested that the intensity records from JTWC are relatively reliable. Recently, *Wu and Zhao* [2012] compared the dynamically derived intensity records to those from the three best track data sets including JTWC, CMA_STI, and JMA and found that the TC intensity data from JTWC is more reliable than the other two best track data sets. To further enhance our analyses, we used the three best track data sets available from the JTWC, CMA_STI, and JMA and found consistent results for the two record low TC genesis frequencies in 2010 and 1998. In this study, we mainly focus on the JTWC best track data set.

To examine the impact of large-scale fields on the lowest TC activity during the late-season in 2010 and 1998, the environmental variables (i.e., air temperature, relative humidity, specific humidity, wind fields) in this study are taken from the National Centers for Environmental Prediction and National Center for Atmospheric Research (NCEP/NCAR) Reanalysis I data set [*Kalnay et al*., 1996] at a 2.5° × 2.5° grid. The SST data are from the National Oceanic and Atmospheric Administration (NOAA) extended reconstructed SST (ERSST version 3) data with 2° latitude by longitude 2° resolution [*Smith and Reynolds*, 2004].

2.2. Genesis Potential Index

To explore key factors affecting the extremely low TC activity in 2010 and 1998, the genesis potential index (GPI) developed by *Emanuel and Nolan* [2004] is adopted in this study. The GPI is defined on the basis of the four factors:

$$\mathrm{GPI}=|10^5\eta|^{\frac{3}{2}}\left(\frac{H}{50}\right)^3\left(\frac{V_{\mathrm{pot}}}{70}\right)^3(1+0.1V_{\mathrm{shear}})^{-2}, \tag{1}$$

where η is the absolute vorticity at 850 hPa (s^{-1}), H is the relative humidity (RH) at 600 hPa (%), V_{pot} is the potential intensity (PI) (m s^{-1}), and V_{shear} is calculated as the magnitude of the difference of wind vectors (m s^{-1}) between 850 and 200 hPa. The PI is obtained from SST, sea level pressure, and vertical profiles of atmospheric temperature and humidity using a technique that is a generalization of that described in *Emanuel* [1995] to take into account dissipative heating. The PI can be computed according to the algorithm of *Bister and Emanuel* [2002], who consider SST and vertical profiles of temperature and specific humidity in the troposphere and define V_{pot} as

$$V_{\mathrm{pot}}{}^2=\frac{T_s}{T_o}\frac{C_k}{C_D}(CAPE^*-CAPE^b), \tag{2}$$

where T_s is SST, T_o is the mean outflow temperature at the level of neutral buoyancy, C_k is the exchange coefficient for enthalpy, C_D is the drag coefficient, $CAPE^*$ is the convective available potential energy (CAPE) with reference to environmental sounding, and $CAPE^b$ is CAPE of the boundary layer air.

2.3. MRI-AGCM 3.2 Model

To understand how the regional SST anomalies modulate the critical circulation conditions that affect the TC genesis in the late-season of 2010 and 1998, a new version of the atmospheric general circulation model

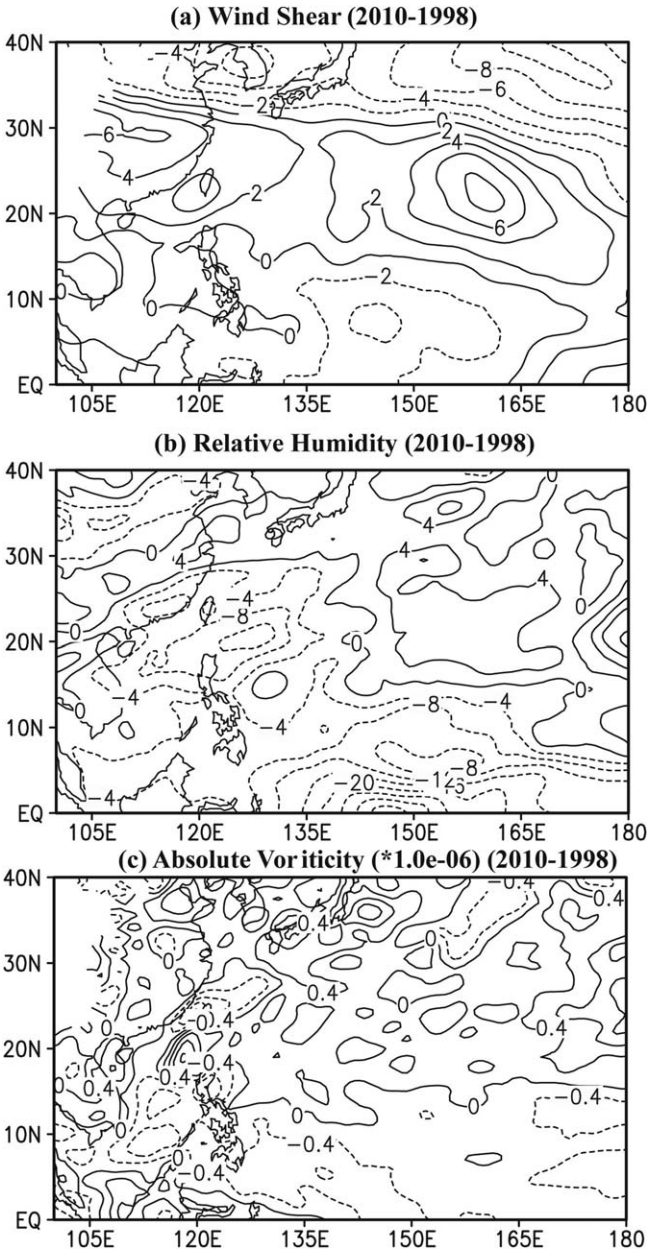

Figure 7. Observed differences (i.e., 2010 minus 1998) of vertical wind shear, 600 hPa relative humidity, and absolute vorticity at 850 hPa during the late-season.

(AGCM) from the Meteorological Research Institute at TL95 resolution (~180 km) (referred to as MRI-AGCM 3.2 model) with an upgraded Yoshimura cumulus scheme forced by different boundary conditions is used. Compared to the previous version, the new MRI-AGCM 3.2 model substantially improves the simulations of large-scale circulations and precipitation [*Mizuta et al*., 2012; *Sugi et al*., 2012], as well as the distribution and intensity of TCs [*Murakami et al*., 2013a, 2013b]. Details of the model description and performance can be found in *Mizuta et al*. [2012] and *Yoshimura et al*. [2014].

3. Diagnosis of Key Factors Affecting the Lowest TC Genesis in 2010

Previous studies illustrated that the GPI is able to replicate the observed climatological annual cycle, as well as the interannual variation of TC genesis, in several different basins. Based upon analyses of anomalous GPI by varying variables included in GPI, *Camargo et al*. [2007] examined how different environmental factors contribute to the influence of ENSO on TC activity and found that specific factors have more influence than others in different basins. For example, the midlevel relative humidity (RH) and vertical wind shear (VWS) are important for the reduction in TC genesis over the Atlantic basin during El Niño years, while midlevel RH and low-level vorticity are important for the eastward shift in the mean TC formation location over the WNP basin. *Camargo et al*. [2007] used the first-position density field to represent TC genesis frequency over the globe with nine grid point smoothing. Because of the small domain of the SCS in this study, we will analyze the actual TC genesis location and GPI in a uniform 2.5° resolution latitude-longitude grid box without spatial smoothing during the late-season for 2010 and 1998.

To assess the environmental factors that characterize the low TC genesis, we first calculate the monthly GPI anomaly (difference from monthly climatology) for the period 1979–2012. From these anomalies, we obtain the anomaly composite in the late-season for 2010 and 1998. The spatial distribution of the GPI anomalies is marked by negative anomalies over the SCS in the late-season of 2010 (Figure 4a) and positive anomalies over the SCS in the late-season of 1998 (Figure 4b). This is consistent with the decreased TC number in the late-season of 2010 (zero TCs) and the increased TC number in the late-season of 1998 (four TCs). In Figure 4c, negative GPI anomalies extend from the SCS southeastward through Palau to the equatorial western Pacific near 140°E. For simplicity, this band of negative GPI anomalies is referred to as the SCS-EWP

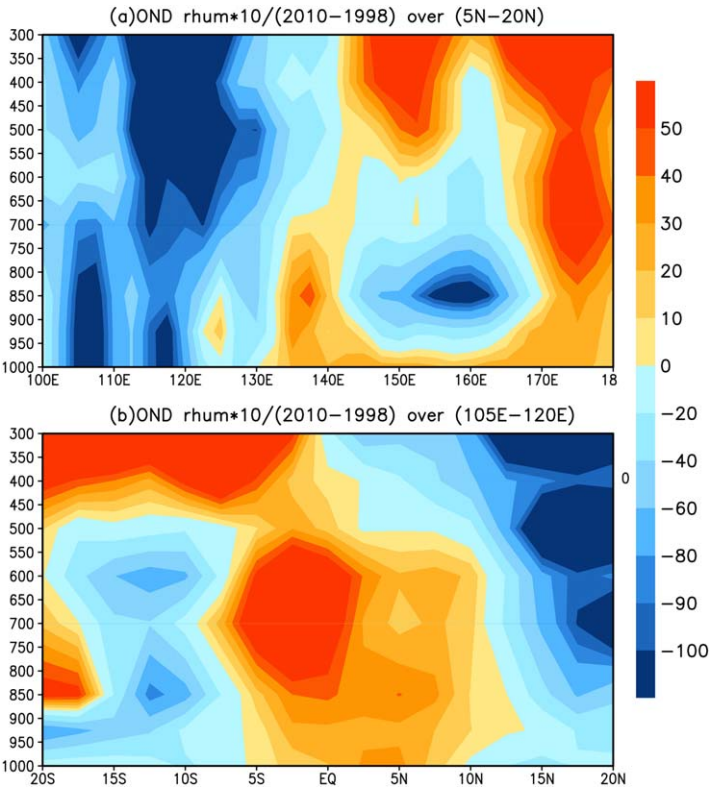

Figure 8. The difference in relative humidity during the late-season between 2010 and 1998: (a) zonal-vertical cross section over 7°N–16°N and (b) the meridional-vertical cross section over 105°E–120°E.

hereafter. Positive GPI anomalies are observed to the east of Philippines. The aforementioned feature characterized by GPI is consistent with the observed differences in TC activity over the SCS region between 2010 and 1998.

To understand the physical processes for the record low TC genesis during the late-season in 2010 and 1998, we examine the individual roles of the four variables that comprise the GPI, including vorticity, VWS, PI, and RH. We calculate the GPI using the long-term climatology (1979–2012) of three of the four variables while keeping the fourth variable to the actual value in 2010 and 1998. This is then repeated for each of the other three variables. The anomalies in 2010 and 1998 are then recalculated in all four cases. Due to the nonlinearity of the GPI, the net anomaly cannot be simply described as the sum of the four fields described here. Nevertheless, to a certain extent, the index can provide weights that appropriately quantify the roles of the different factors in TC genesis provided that the nonlinearities are not too large [*Camargo et al*., 2007].

Figure 5 shows the difference in GPI anomalies between 2010 and 1998 in the late-season in the case of varying VWS (Figure 5a), PI (Figure 5b), RH (Figure 5c), and vorticity (Figure 5d). In each case, the other three variables are fixed at their long-term climatological values. Comparing this with the pattern obtained when all four factors vary (Figure 4c), the decrease in the GPI anomalies in the SCS-EWP appears to be due to the combined changes in VWS, PI, RH, and low-level vorticity. The pattern correlation of the total GPI anomalies and the GPI anomalies with varying VWS is 0.78, varying PI 0.70, varying RH 0.73, and varying low-level vorticity 0.79 over the WNP basin. These correlation coefficients are significant at the 95% confidence level. Similar results can also found over the SCS region. In an operational setting, a pattern correlation of 0.60 is deemed as a lower limit for field forecasts that are synoptically useful. Where the changes in TC numbers and GPI are most pronounced for the SCS during the two extreme years, further investigation based on the reanalysis is performed to examine the role of the aforementioned four factors in possibly modulating TC frequency. This is carried out by examining the contribution of each individual factor to the total GPI anomalies over the SCS region. As shown in Figure 6, decreased low-level absolute vorticity plays a largest role in contributing to the total GPI anomalies over the SCS, and the second contribution comes from the enhanced VWS, with relatively small contributions from the negative PI and the decreased RH.

Figure 7 displays the difference in VWS, RH, and low-level vorticity over the WNP and SCS between 2010 and 1998. The increase in VWS of about 1–2 m s^{-1} is observed over the SCS (Figure 7a) and thus should physically decrease TC formation to some extent as the vertical wind shear is one of the major factors affecting the development of tropical synoptic-scale disturbances and, thus, TC formation [*McBride and Zehr*, 1981; *Molinari et al*., 2004]. Meanwhile, the large decrease in the midlevel RH is found over the tropical WNP and particularly over the SCS-EWP when 2010 is compared to 1998 (Figures 7b and 8). This decline in RH over the SCS (110–120°E) is deep in the troposphere (Figure 8a). In Figure 7c, the region of decreased low-

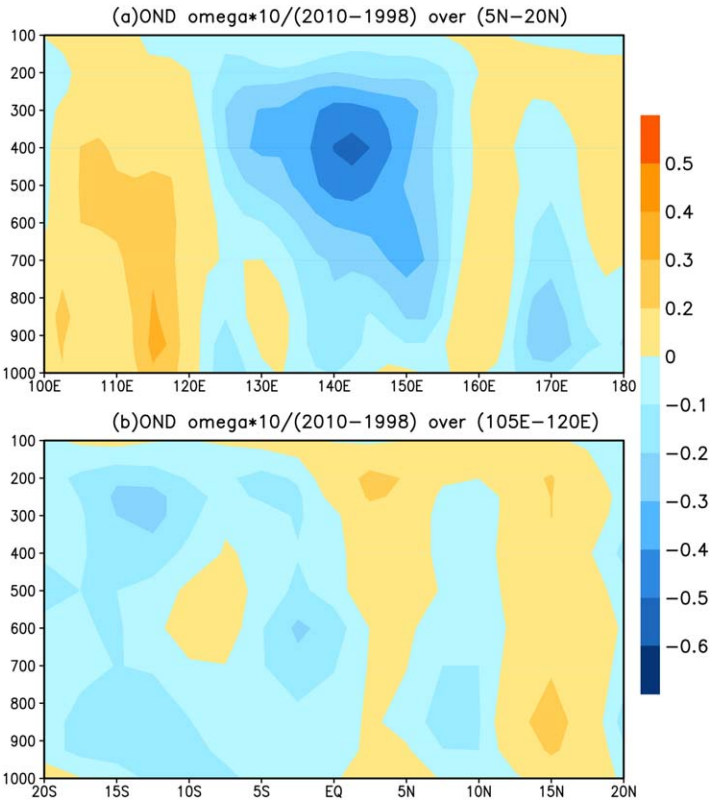

Figure 9. The difference of omega during the late-season between 2010 and 1998: (a) zonal-vertical cross section over 7°N–16°N and (b) the meridional-vertical cross section over 105°E–120°E. The unit is 0.1 Pa/s.

level vorticity is more significant and is confined mainly near the East China Sea and the SCS-EWP. Moreover, changes in PI (not shown) are generally consistent with the cooling SST over the WNP basin in 2010 compared to that in 1998 (Figure 2c).

For the vertical motion field, an area of subsidence anomaly over the SCS between 110–120°E related to the cold SST anomaly (Figure 2c) is observed (Figure 9a). A deep vertical layer of subsidence anomaly also occurs over the area centered around 15°N in the meridional-vertical cross section (Figure 9b), while an ascending anomaly can be observed between 5°N and 10°N. Considering the SCS as a whole region, the subsidence anomaly is evident in 2010. Associated with the subsidence anomaly, the anticyclonic circulation anomaly prevails over the SCS, as evident by the decreased absolute vorticity (Figure 7c). Taken together, these large-scale conditions are more unfavorable for TC genesis in 2010 late-season over the SCS than in 1998. The remarkable decrease in TC frequency during the late-season in 2010 over the SCS is mainly accompanied by the decrease in low-level relative vorticity and an enhancement in VWS.

4. Role of Regional SST Changes in the TC Genesis Frequency

The extremely low TC activity during the late-season in 2010 may be associated with the atmospheric circulation in response to the tropics-wide SST change. Previous studies suggested that the cooling in the WNP basin contributes negatively to the TC activity through the local thermodynamic process (a negative PI anomaly) [*Emanuel*, 1987; *Knutson et al*., 1998; *Knutson and Tuleya*, 2004]. Moreover, the SST anomaly associated with a La Niña-like pattern could induce significant dynamical controls to the TC genesis change [*Emanuel*, 1987; *Wu and Lau*, 1992]. In addition to the SST anomaly in the Pacific, the SST anomaly in the Indian Ocean can also affect TC frequency over the WNP and SCS by means of modulating the monsoon circulation and the equatorial Kelvin wave activity [*Zhan et al*., 2011; *Du et al*., 2011; *Tao et al*., 2012]. To further elucidate how the SST over different basins may exert dynamical control over the TC genesis during the late-season, a suite of AGCM experiments is carried out.

The lower boundary conditions for the MRI-AGCM are illustrated in Figure 10. In the control experiment, referred to as EXP_CNTL, the global late-season mean SST in 1998 is used (Figure 10a). To examine the impacts of the tropical SST anomaly between the two extreme years, the experiment is forced with global SST used in the control run plus the SST difference between the 2 years (i.e., 2010 minus 1998) over the globe, referred to as the experiment EXP_All (Figure 10b). This experiment (EXP_All) is designed to determine if the changes to large-scale circulation and GPI are related to the global SST difference between 2010 and 1998.

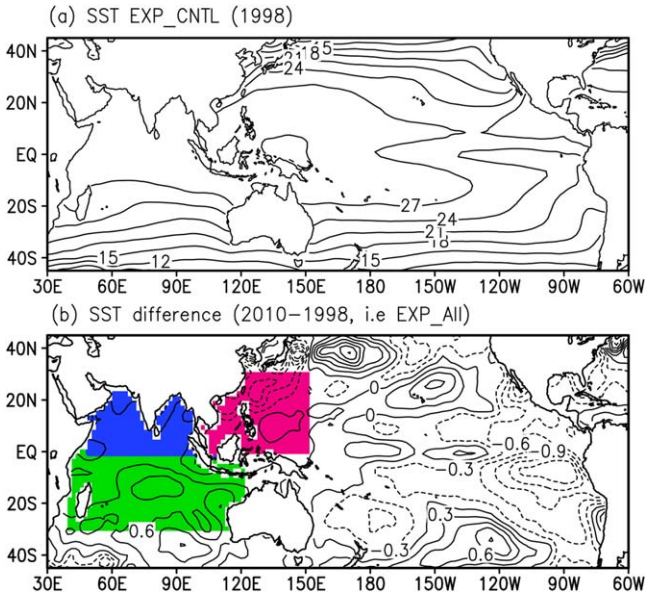

Figure 10. (a) Sea surface temperatures during the late-season of 1998 for the EXP_CNTL (°C). (b) Tropical SST anomalies (2010 minus 1998, °C) during the late-season that are added onto the SST in the EXP_CNTL to force the AGCM in the various experiments (red for the EXP_WP, green for the EXP_SIO, blue for the EXP_NIO, and the global SST anomalies altogether for the EXP_All).

To pinpoint the relative roles of local-versus-remote SST anomalies to the changes in TC genesis frequency during the late-season between 2010 and 1998, three additional individual experiments are conducted. Figure 10b shows data for the three different basins forced with the SST in the control run along with SST difference (i.e., 2010 minus 1998). The three experiments are referred to as EXP_WP, EXP_SIO, and EXP_NIO, respectively.

To enhance the results, the ensemble simulations with initial conditions on the 1st of November for five different years are performed, as in *Hsu et al*. [2014]. The solar radiation at the top of the atmosphere is fixed at the same level as the 1st of November to represent the late-season conditions. All of the simulations are integrated for a period of 10 years after an initial spin-up of a few months. The simulated results shown here are averages of five ensemble runs for each experiment.

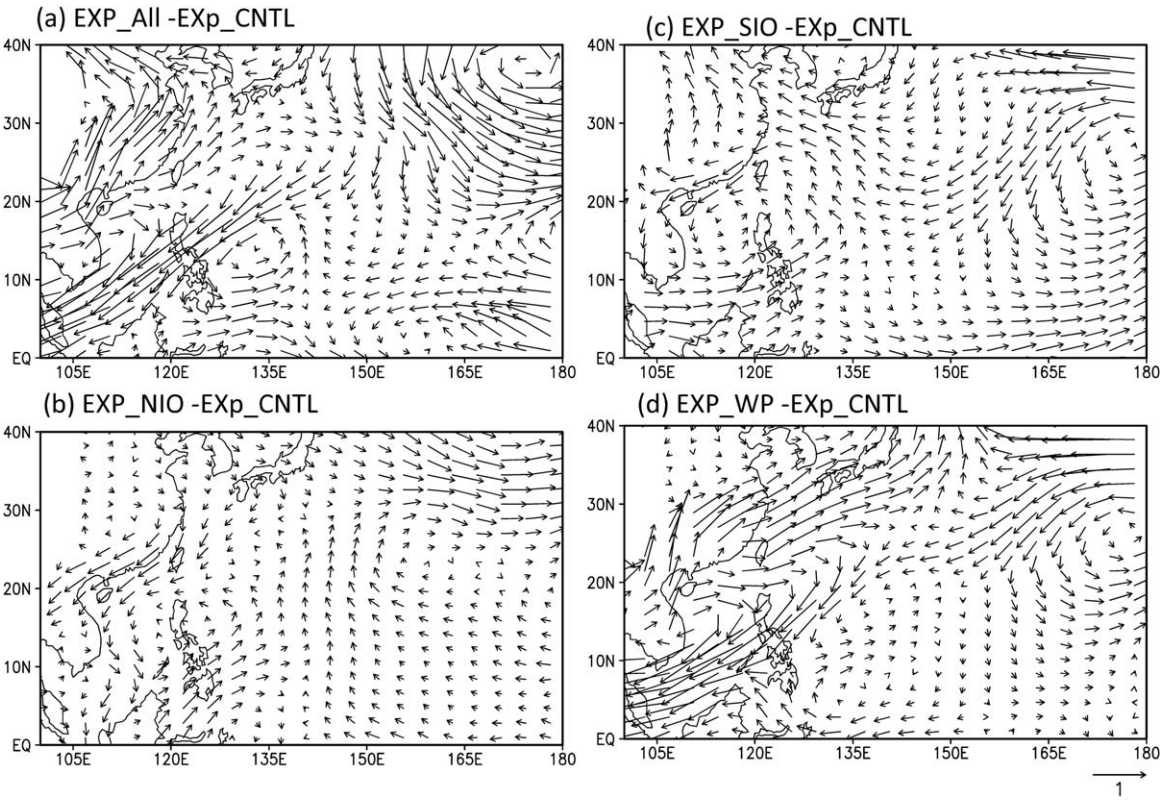

Figure 11. Simulated deviations of 850 hPa wind in EXP_ALL, EXP_NIO, EXP_SIO, and EXP_WP from EXP_CNTL.

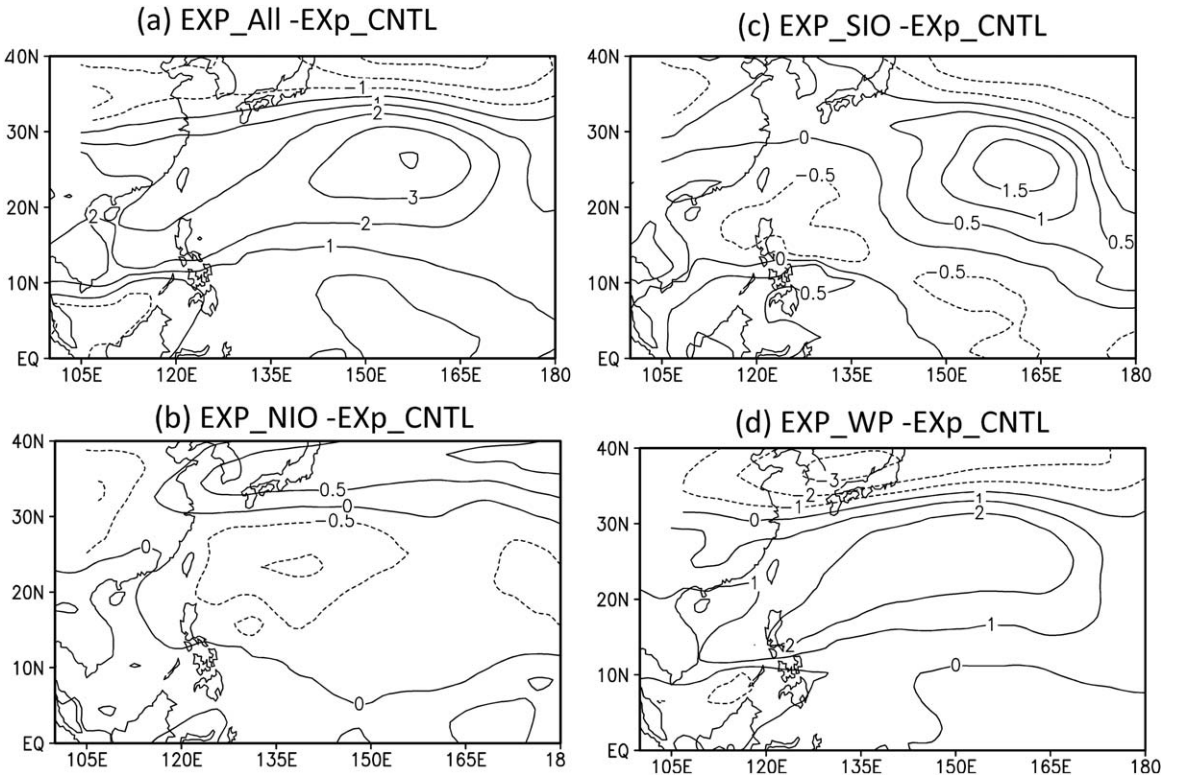

Figure 12. Same as in Figure 11 but for the vertical wind shear, which is computed as the difference of wind between 850 and 200 hPa.

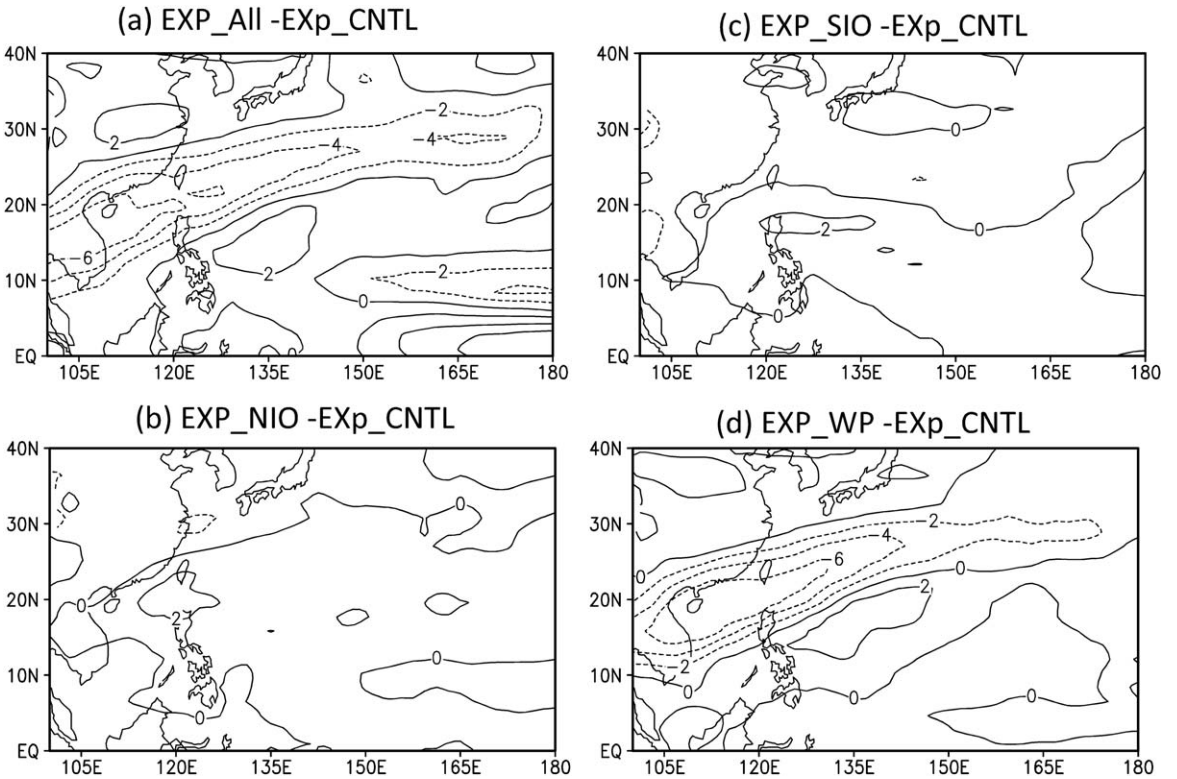

Figure 13. Same as in Figure 11 but for 600 hPa relative humidity.

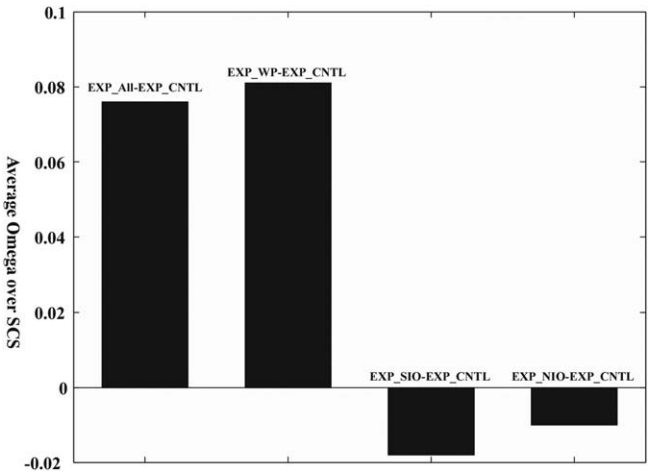

Figure 14. Averaged omega deviations at 500 hPa over the SCS region for (a) EXP_All, (b) EXP_WP, (c) EXP_SIO, and (d) EXP_NIO from EXP_CNTL, respectively. The unit is Pa/s.

Next we turned our attention to the role of SST forcing in the WNP basin and the Indian Ocean to TC activity. Figure 11 shows the simulated deviations of the late-season wind fields at 850 hPa in (a) EXP_All, (b) EXP_NIO, (c) EXP_SIO, and (d) EXP_WP from EXP_CNTL, respectively. These represent changes in the lower-troposphere circulation due to ocean boundary forcing. As shown in Figure 11a, the model realistically simulates the main features of the low-level wind vector difference (i.e., 2010 minus 1998) with the anticyclonic circulation over the SCS and Philippines (Figure 7c). The anticyclonic circulation anomaly is also captured in the EXP_WP run (Figure 11d). The anomalous anticyclone over the SCS implies a decrease in the low-level vorticity, which is unfavorable for TC formation [*Gray*, 1968; *Vitart et al*., 1999]. For the EXP_NIO and EXP_SIO runs, an anomalous cyclone is present over the SCS (Figures 11b and 11c). This feature is inconsistent with observations. These results suggest that the observed anticyclonic anomalies over the SCS and Philippines (i.e., 2010 minus 1998) occur mainly from the regional SST change in the WNP basin. For the VWS, the simulated differences in the late-season for EXP_All, EXP_SIO, EXP_NIO, and EXP_WP from EXP_CNTL are shown in Figure 12. An increase in VWS is noted in the northern SCS and a small decrease in VWS is observed over the southern SCS in EXP_ALL experiment (Figure 12a). This pattern is in similar to that in EXP_WP (Figure 12d). For the EXP_NIO and EXP_SIO runs, the pattern of VWS over the SCS is almost the opposite of that in EXP_All (Figures 12b and 12c).

Figure 13 displays simulated deviations of the late-season mean RH at 600 hPa in (a) EXP_All, (b) EXP_NIO, (c) EXP_SIO, and (d) EXP_WP from EXP_CNTL, respectively. In association with the anomalous anticyclone (Figures 11a and 11d) and suppressed TC formation (Figure 3), there are negative RH anomalies at 600 hPa over the SCS in the EXP_ALL and EXP_WP (Figures 13a and 13d) experiments, but a positive one in EXP_NIO and EXP_SIO (Figures 13b and 13c) over the same region. Further examinations indicate that the decreased (increased) RH is associated with the decreased (enhanced) upward vertical motion over the SCS (Figure 14), which may be responsible for the decreased (increased) midlevel RH by suppressing (enhancing) the vertical transport of moisture flux [*Wu et al*., 2010]. Meanwhile, the most significant subsidence appears in EXP_All and EXP_WP, but a moderate upward motion can also be observed in EXP-SIO and EXP_NIO, again suggesting the dominant role of the WNP SST change in 2010 that produced an unfavorable environment for TC development over the SCS.

In summary, the regional SST anomalies in 2010 over the WNP basin, which is characterized by less warming when compared to 1998, induce an anomalous low-level anticyclone over the SCS compared to that in 1998. This leads to a decrease in upward motion and midlevel RH and to an increase in VWS, which reduces TC formation over the SCS region. The effect of regional SST distribution on the SIO and NIO, however, is the opposite because of the induced upward motion and enhanced RH in the middle troposphere. These results indicate that the relatively suppressed TC formation over the SCS region in the late-season of 2010 mainly results from the WNP regional SST change. This effect is partly offset by the regional SST distribution over the SIO and NIO. Similar to the observation analyses, GPI analyses based on the model data reveal that all four factors contribute to the lowest TC genesis during the late-season in 2010 over the SCS region. The decreased low-level absolute vorticity plays the most important role, followed by the enhanced VWS (figures not shown).

5. Summary

The annual TC number in the WNP and SCS regions is characterized by a record low value in 2010, followed by 1998. The TC genesis frequency during the 2010 peak season (July to September) is slightly higher than

in 1998 (11 TCs versus 9). For the late-season (October to December), eight TCs occurred in 1998 but only two in 2010, which makes the entire year of 2010 inactive. During the late-season, there were four TCs generated over the SCS in 1998, but not a single one over the same region in the late-season of 2010. Large-scale environmental conditions instrumental for TC occurrence during the late-season of 2010 are contrasted to those in 1998 using the NCEP/NCAR reanalysis data sets and numerical experiments with a state-of-the-art MRI-AGCM model.

The GPI analysis suggests that the lower TC frequency in 2010 relative to 1998 during the late-season results mainly from unfavorable environmental conditions including lower RH in the middle troposphere, enhanced VWS, negative anomalies in PI, and decreased low-level absolute vorticity. For the SCS, low-level vorticity plays the most important role in contributing to the lowest TC frequency in 2010, followed by the VWS, midlevel humidity, and PI. Results from numerical simulations support the relative roles of the aforementioned four factors found in observation. Further examinations based on numerical experiments suggest that the sharply decreased TC formation over the SCS in 2010 mainly results from the WNP regional SST anomaly, and its effect is partly offset by the SST anomaly in the SIO and NIO basins. The regional SST distribution in 2010 over the WNP basin induces an anomalous low-level anticyclone in the SCS, leading to a decrease in low-level vorticity, reduction in vertical motion and midlevel RH, and an enhancement in VWS. All of these conditions lead to a reduction in TC formation over the SCS region, more during the 2010 late-season than in 1998. This study provides better understanding of mechanisms of low TC activity over the WNP basin, which could benefit climate prediction of TC activity by operational centers.

Acknowledgments

The TC data are available from the JTWC (http://jtwccdn.appspot.com/NOOC/nmfc-ph/RSS/jtwc/best_tracks/wpindex.php), the environmental variables data from NCEP/NCAR (http://www.esrl.noaa.gov/psd/data/gridded/data.ncep.reanalysis.derived.surface.html), and SST data from NOAA (http://www.esrl.noaa.gov/psd/data/gridded/data.noaa.ersst.html). This research is jointly supported by the National Natural Science Foundation of China (grant 41305050, 41275093, and 41475091), the National Basic Research Program of China (2013CB430103, 2015CB452803), the project of the specially appointed professorship of Jiangsu Province, and the Priority Academic Program Development of Jiangsu Higher Education Institutions (PAPD). P.-C. Hsu is supported by the NSFC (grant 41375100), the Natural Science Foundation of the Jiangsu Province, China (BK20140046), and the Research Project of Chinese Ministry of Education (213014A). H.M. was supported by the SOUSEI program of the Ministry of Education, Culture, Sports, Science, and Technology (MEXT) of Japan. The model simulations were performed on the Earth Simulator. This study is the Earth System Modeling Center Contribution Number 021.

References

Bister, M., and K. A. Emanuel (2002), Low frequency variability of tropical cyclone potential intensity I. Interannual to interdecadal variability, *J. Geophys. Res.*, *107*(D24), 4801, doi:10.1029/2001JD000776.

Camargo, S. J., and A. H. Sobel (2005), Western North Pacific tropical cyclone intensity and ENSO, *J. Clim.*, *18*, 2996–3006.

Camargo, S. J., K. A. Emanuel, and A. H. Sobel (2007), Use of a genesis potential index to diagnose ENSO effects on tropical cyclone genesis, *J. Clim.*, *20*, 4819–4834.

Chan, J. C. L. (1985), Tropical cyclones activity in the northwest Pacific in relation to the El Niño/Southern Oscillation phenomenon, *Mon. Weather Rev.*, *113*, 599–606.

Chan, J. C. L. (2000), Tropical cyclone activity over the western North Pacific associated with El Niño and La Niña events, *J. Clim.*, *13*, 2960–2972.

Chan, J. C. L. (2008), Decadal variations of intense typhoon occurrence in the western North Pacific, *Proc. R. Soc. A*, *464*, 249–272.

Chen, T. C., and S. P. Weng (1998), Interannual variation of the summer synoptic-scale disturbances activity in the western Tropical Pacific, *Mon. Weather Rev.*, *126*, 1725–1733.

Chia, H. H., and C. F. Ropelewski (2002), The interannual variability in the genesis location of tropical cyclones in the northwest Pacific, *J. Clim.*, *15*, 2934–2944.

Chu, P.-S. (2004), ENSO and tropical cyclone activity, in *Hurricanes and Typhoons, Past, Present and Future*, edited by R. J. Murnane and K.-B. Liu, pp. 297–332, Columbia Univ. Press, N. Y.

Dong, K. (1988), El Niño and tropical cyclone frequency in the Australian region and the northwest Pacific, *Aust. Meteorol. Mag.*, *36*, 219–225.

Du, Y., L. Yang, and S. P. Xie (2011), Tropical Indian Ocean influence on Northwest Pacific tropical cyclones in summer following strong El Niño, *J. Clim.*, *24*, 315–322.

Emanuel, K., R. Sundararajan, and J. Williams (2008), Hurricanes and global warming: Results from downscaling IPCC AR4 simulations, *Bull. Am. Meteorol. Soc.*, *89*, 347–367.

Emanuel, K. A. (1995), Sensitivity of tropical cyclones to surface exchange coefficients and a revised steady-state model incorporating eye dynamics, *J. Atmos. Sci.*, *52*, 3969–3976.

Emanuel, K. A. (1987), The dependence of hurricane intensity on climate, *Nature*, *326*, 483–485.

Emanuel, K. A. (2005), Increasing destructiveness of tropical cyclones over the past 30 years, *Nature*, *436*, 686–688.

Emanuel, K. A., and D. S. Nolan (2004), Tropical cyclone activity and the global climate system, in *Proceedings of the 26th Conference on Hurricanes and Tropical Meteorology, Am. Meteorol. Soc.*, Miami, Fla.

Gray, W. M. (1968), Global view of the origin of tropical disturbances and storms, *Mon. Weather Rev.*, *96*, 669–700.

Ho, C.-H., J.-J. Baik, J.-H. Kim, D.-Y. Gong, and C.-H. Sui (2004), Inter-decadal changes in summertime typhoon tracks, *J. Clim.*, *17*, 1767–1776.

Hsu, P.-C., P.-S. Chu, H. Murakami, and X. Zhao (2014), An abrupt decrease in the late-season typhoon activity over the western North Pacific, *J. Clim.*, *27*, 4296–4312.

Huang, P., C. Chou, and R. Huang (2011), Seasonal modulation of tropical intraseasonal oscillations on tropical cyclone geneses in the western North Pacific, *J. Clim.*, *24*, 6339–6352.

Kalnay, E., et al. (1996), The NCEP/NCAR 40-year reanalysis project, *Bull. Amer. Meteor. Soc.*, *77*, 437–471.

Kamahori, H. N., N. Yamazaki, N. Mannoji, and K. Takahashi (2006), Variability in intense tropical cyclone days in the western North Pacific, *SOLA*, *2*, 104–107, doi:10.2151/sola.2006-027.

Kim, J., C. Ho, H. Kim, C. Sui, and K. Seon (2008), Systematic variation of summertime tropical cyclone activity in the western North Pacific in relation to the Madden-Julian oscillation, *J. Clim. 21*, 1171–1191.

Knutson, T. R., and R. E. Tuleya (2004), Impact of CO_2-induced warming on simulated hurricane intensity and precipitation: Sensitivity to the choice of climate model and convective parameterization, *J. Clim.*, *17*, 3477–3495.

Knutson, T. R., R. E. Tuleya, and Y. Kurihara (1998), Simulated increase of hurricane intensities in a CO_2-warmed climate, *Science*, *279*, 1018–1021.

Knutson, T. R., J. J. Sirutis, S. T. Garner, G. A. Vecchi, and I. M. Held (2008), Simulated reduction in Atlantic hurricane frequency under twenty-first-century warming conditions, *Nat. Geosci.*, *1*, 359–364.
Lander, M. A. (1994), An exploratory analysis of the relationship between tropical storm formation in the western North Pacific and ENSO, *Mon. Weather Rev.*, *122*, 636–651.
Latif, M., N. Keenlyside, and J. Bader (2007), Tropical sea surface temperature, vertical wind shear, and hurricane development, *Geophys. Res. Lett.*, *34*, L01710, doi:10.1029/2006GL027969.
Li, R. C. Y., and W. Zhou (2013), Modulation of western north Pacific tropical cyclone activity by the ISO. Part I: Genesis and intensity, *J. Clim.*, *26*, 2904–2918.
Liebmann, B., H. H. Hendon, and J. D. Glick (1994), The relationship between tropical cyclones of the western Pacific and Indian Oceans and the Madden-Julian Oscillation, *J. Meteorol. Soc. Jpn.*, *72*, 401–412.
Liu, K. S., and J. C. L. Chan (2008), Interdecadal variability of western North Pacific tropical cyclone tracks, *J. Clim.*, *21*, 4464–4476.
Liu, K. S., and J. C. L. Chan (2013), Inactive period of western North Pacific tropical cyclone activity in 1998–2011, *J. Clim.*, *26*, 2614–2630.
Maue, R. N. (2011), Recent historically low global tropical cyclone activity, *Geophys. Res. Lett.*, *38*, L14803, doi:10.1029/2011GL047711.
McBride, J. L., and R. Zehr (1981), Observational analysis of tropical cyclone formation: Comparison of non-developing versus developing systems, *J. Atmos. Sci.*, *38*, 1132–1151.
Mizuta, R., et al. (2012), Climate simulations using the improved MRI-AGCM with 20-km grid, *J. Meteorol. Soc. Jpn.*, *90A*, 233–258, doi: 10.2151/jmsj.2012-A12.
Molinari, J., D. Vollaro, and K. L. Corbosiero (2004), Tropical cyclone formation in a sheared environment: A case study, *J. Atmos. Sci.*, *61*, 2493–2509.
Murakami, H., B. Wang, T. Li, and A. Kitoh (2013a), Projected increase in tropical cyclones near Hawaii, *Nat. Clim. Change*, *3*, 749–754, doi: 10.1038/nclimate1890.
Murakami, H., M. Sugi, and A. Kitoh (2013b), Future changes in tropical cyclone activity in the North Indian Ocean projected by high-resolution MRI-AGCMs, *Clim. Dyn.*, *40*(7–8), 1949–1968.
Ren, F., J. Liang, G. Wu, W. Dong, and X. Yang (2011), Reliability analysis of climate change of tropical cyclone activity over the western North Pacific, *J. Clim.*, *24*, 5887–5898.
Smith, T. M., and R. W. Reynolds (2004), Improved extended reconstruction of SST (1854–1997), *J. Clim.*, *16*, 149–1510.
Song, J.-J., Y. Wang, and L. Wu (2010), Trend discrepancies among three best track data sets of western North Pacific tropical cyclones, *J. Geophys. Res.*, *115*, D12128, doi:10.1029/2009JD013058.
Sugi, M., H. Murakami, and J. Yoshimura (2012), On the mechanism of tropical cyclone frequency changes due to global warming, *J. Meteorol. Soc. Jpn.*, *90A*, 397–408, doi:10.2151/jmsj.2012-A24.
Tao, L., L. Wu, Y. Wang, and L. Yang (2012), Influence of tropical Indian Ocean warming and ENSO on tropical cyclone activity over the western North Pacific, *J. Meteorol. Soc. Jpn.*, *90*, 127–144.
Vecchi, G. A., and B. J. Soden (2007), Increased tropical Atlantic wind shear in model projections of global warming, *Geophys. Res. Lett.*, *34*, L08702, doi:10.1029/2006GL028905.
Vitart, F., J. L. Anderson, and W. F. Stern (1999), Impact of large-scale circulation on tropical storm frequency, intensity, and location, simulated by an ensemble of GCM integrations, *J. Clim.*, *12*, 3237–3254.
Wang, B., and J. C. Chan (2002), How strong ENSO events affect tropical storm activity over the western North Pacific, *J. Clim.*, *13*, 1517–1536.
Wu, G., and N.-C. Lau (1992), A GCM simulation of the relationship between tropical storm formation and ENSO, *Mon. Weather Rev.*, *120*, 958–977.
Wu, L., and B. Wang (2008), What has changed the proposition of intense hurricanes in the last 30 years?, *J. Clim.*, *21*, 1432–1439.
Wu, L., and H. Zhao (2012), Dynamically derived tropical cyclone intensity changes over the western North Pacific, *J. Clim.*, *25*, 89–98.
Wu, L., L. Tao, and Q. Ding (2010), Influence of sea surface warming on environmental factors affecting long-term changes of Atlantic tropical cyclone formation, *J. Clim.*, *23*, 5978–5989.
Wu, M.-C., K.-H. Yeung, and W.-L. Chang (2006), Trends in western North Pacific tropical cyclone intensity, *Eos Trans. AGU*, *87*, 537–538.
Yokoi, S., and Y. N. Takayabu (2013), Attribution of decadal variability in tropical cyclone passage frequency over the western North Pacific: A new approach emphasizing the genesis place of cyclones, *J. Clim.*, *26*, 973–987, doi:10.1175/JCLI-D-12-00060.1.
Yoshimura, H., R. Mizuta, and H. Murakami (2014), A spectral cumulus parameterization scheme interpolating between two convective updrafts with semi-Lagrangian calculation of transport by compensatory subsidence, *Mon. Weather Rev.*, doi:10.1175/MWR-D-14-00068.1.
Yumoto, M., and T. Matsuura (2001), Interdecadal variability of tropical cyclone activity in the western North Pacific, *J. Meteorol. Soc. Jpn.*, *79*, 23–25.
Yumoto, M., T. Matsuura, and S. Lizuka (2003), Interdecadal variability of tropical cyclone frequency over the western North Pacific in a high-resolution atmosphere-ocean coupled GCM, *J. Meteorol. Soc. Jpn.*, *81*, 1069–1086.
Zhan, R., Y. Wang, and X. Lei (2011), Contributions of ENSO and east Indian Ocean SSTA to the interannual variability of Northwest Pacific tropical cyclone frequency, *J. Clim.*, *24*, 509–521.
Zhao, H., L. Wu, and W. Zhou (2010), Assessing the influence of the ENSO on tropical cyclone prevailing tracks in the western North Pacific, *Adv. Atmos. Sci.*, *27*, doi:10.1007/s00376-010-9161-9.
Zhao, H., L. Wu, and W. Zhou (2011), Interannual changes of tropical cyclone intensity in the western north Pacific, *J. Meteorol. Soc. Jpn.*, *89*(3), 243–253, doi:10.2151/jmsj.2011-305.
Zhao, H., L. Wu, and R. Wang (2014), Decadal variations of intense tropical cyclones over the Western North Pacific during 1948–2010, *Adv. Atmos. Sci.*, *31*(1), 57–65, doi:10.1007/s00376-013-3011-5.